

Efficient photodegradation of Acid Red B by immobilized ferrocene in the presence of UVA and H₂O₂

Yulun Nie, Chun Hu*, Jiuhui Qu, Xuexiang Hu

*State Key Laboratory of Environmental Aquatic Chemistry, Research Center for Eco-Environmental Sciences,
Chinese Academy of Sciences, Beijing 100085, China*

Received 3 April 2007; received in revised form 4 September 2007; accepted 4 October 2007

Available online 7 October 2007

Abstract

SiO₂-C₂H₄-ferrocene (SiCFe) was synthesized by covalent grafting of ferrocene on functionalized silica gel with a -C₂H₄- linkage. On the basis of characterization by diffuse reflectance UV-vis spectra (DRS) and Fourier transform infrared spectra (FT-IR), ferrocene has been successfully anchored on the silica gel. Under UVA ($\lambda_{\text{max}} = 365 \text{ nm}$) irradiation, the catalyst exhibited high photocatalytic activity in the degradation of Acid Red B (ARB), especially in the presence of H₂O₂. Meanwhile, the catalytic activity of SiCFe was maintained effectively even after reused for 4 times without any significant destruction of ferrocene. The influence of initial solution pH and wavelength of UV light on the catalyst's activity was also investigated. Electron spin resonance (ESR) studies revealed that both $\cdot\text{OH}$ and $\text{HO}_2\cdot/\text{O}_2^{\cdot-}$ radicals were involved as the active species in the ARB degradation process. Furthermore, results of total organic carbon (TOC) and FT-IR analysis indicated that ARB degradation proceeded by the cleavage of -N=N-, followed by hydroxylation and opening of phenyl rings to form aliphatic acids and further oxidation of the aliphatic acids to produce carbon dioxide and water. A possible reaction mechanism was proposed on the basis of all the information obtained under various experimental conditions.

© 2007 Elsevier B.V. All rights reserved.

Keywords: Ferrocene; Silica gel; Covalent grafting; Acid Red B; Photodegradation

1. Introduction

It is known that azo dyes are non-biodegradable compounds existing in a wide concentration range in industrial effluents [1–3], and their release is an important source of esthetic pollution, eutrophication, and perturbations in aquatic life [3]. Apart from the traditional methods of removing these azo dyes, advanced oxidation technologies (AOTs) are innovative methods for treatment of these pollutants to more biodegradable molecules or other inorganics [4,5]. In recent years, various heterogeneous degradation processes based on some metal complexes have been developed. This is due to their unique advantages such as facile catalyst recovery from the solution, physical separation of active sites by dispersion on the supports, significant decrease of the material losses and a lower cost of the wastewater treatment [6,7].

In 1995, Meunier reported for the first time that iron tetra-sulfophthalocyanine supported on ion-exchange resin could efficiently degrade 2,4,6-trichlorophenol in the presence of H₂O₂ [8]. Following this work, many efforts have been made to mimic the catalytic oxidative properties of the enzyme cytochrome P-450 [9,10] and non-heme methane monooxygenase [10–12] for the degradation of organic pollutants. However, these studies are mainly focus on metalphthalocyanine [13,14], metalporphyrin [15,16], metalbipyridine [4,11,17], salen Schiff-base [18], bioactive hemin [12] and their derivatives, and their immobilization is either driven by molecular impregnation [14], template synthesis [19], or flexible ligand route [4,11,15,17]. Due to its high stability, special structure, strong ultraviolet absorbance, ferrocene has wide application in many fields: used in supramolecular chemistry, as magnetic materials and liquid crystals, in asymmetric catalysis, and as oil additives [20–22]. Ferrocene itself can be used as an excellent homogeneous catalyst for benzene and other aromatic compound hydroxylation [23], however, few studies have been conducted to use it as a heterogeneous catalyst for the degradation of azo-dye compounds.

* Corresponding author. Tel.: +86 10 62849628; fax: +86 10 62923541.
E-mail address: huchun@cees.ac.cn (C. Hu).

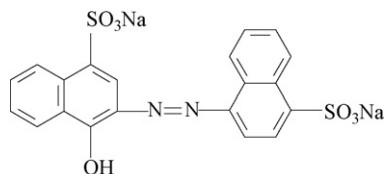


Fig. 1. The structure of Acid Red B.

In this paper, ferrocene was anchored on silica gel by covalent grafting method at ambient conditions, which was different from the reported procedures [23,24]. The catalyst showed high catalytic activity and stability for the degradation of ARB in the presence of H_2O_2 under UVA irradiation. The degradation process was characterized by TOC removal and FT-IR techniques. ESR was used to detect the reactive oxygen species involved in the ARB degradation process. A possible reaction mechanism was proposed.

2. Experimental

2.1. Chemicals

Silica gel (40–80 meshes) was purchased from Qingdao chemical plant. 1,2-Dichloroethane, *N,N*-dimethylformamine, 30 wt.% H_2O_2 (A.R.), and ferrocene (C.R.) were provided by local reagent company. Acid Red B (ARB) was kindly supplied by the Shanghai Chemical Co. and was used without further purification. Its structure was shown further in Fig. 1. The reagent 5,5-dimethyl-1-pyrroline-*N*-oxide (DMPO), used as the spin-trapping agent in ESR studies, was purchased from Sigma Chemical Co. Deionized and doubly distilled water was used throughout this study. NaOH and HCl solutions were used to adjust the pH of the solution.

2.2. Catalyst preparation: immobilization of ferrocene on SiO_2

SiO_2 pretreatment: silica gel was rinsed for 6 h in 6 M HCl solution, washed with water until the effluent was neutral and dried at 70 °C for 24 h.

As shown in Fig. 2, a stoichiometric amount of silica gel was added to 60 ml ethanol containing 3.0 ml 1,2-dichloroethane,

after the addition of pyridine (used as the catalyst), the reaction mixture was refluxed for about 24 h under the nitrogen atmosphere. The suspension was filtered and the solid was washed with ethanol, and dried at 80 °C for 60 min. Then it was added to a solution of 0.8490 g ferrocene and 2.9247 g zinc chloride (used as the catalyst) in 80 ml *N,N*-dimethylformamine, which was refluxed for 24 h. The solvent was removed by filtration and the residue was purified by ethanol till the effluent was clear. After drying at 80 °C for 60 min, a yellow catalyst, abbreviated as $SiO_2-C_2H_4$ -ferrocene (SiCFe), was resulted.

2.3. Procedures and analyses

The light source was a 300-W high-pressure mercury lamp fixed inside a cylindrical Pyrex flask, which was surrounded by a circulating water jacket to cool the lamp. The exterior of the cylindrical Pyrex flask was wrapped by tinfoil, just leaving a small window (3.5 cm × 1.5 cm) at the side face. The light was then focused onto an 80 ml glass reaction vessel. The average light intensity was 14 mW cm⁻². To effectively suspend the catalyst, compressed air was bubbled from the bottom of the reactor. The reaction temperature was maintained at 25 °C.

Unless noted otherwise, 50 mg SiCFe particles were dispersed in 50 ml of dye solution (0.1 mM, ARB, pH = 3.0). Prior to the addition of H_2O_2 and UVA irradiation, the suspensions were stirred in the dark for ca. 10 min to establish adsorption/desorption equilibrium between the dye and the surface of the catalyst. At a given interval of irradiation time, 3-ml samples of the aqueous solutions were filtered through a Millipore filter (pore size 0.45 μm) to remove particles. The filtrates were analyzed by recording variations at the wavelength of maximal absorption ($\lambda = 514$ nm) in the UV-vis spectra of ARB using a 752N spectrophotometer (Shanghai Precision & Scientific Instruments Co., Ltd., China). The total organic carbon (TOC) of the solution was analyzed with a Phoenix 8000 analyzer. The reflectance spectrum (200–800 nm) of the catalyst was recorded on a Hitachi spectrometer, for which $BaSO_4$ was used as the reference. To evaluate the Fe leaching from the catalyst, the Fe concentration in solution was determined by atomic absorption spectrophotometry (AA-6300). The intermediates during the ARB degradation process were recorded by infrared spectra (Nicolet 5700). Samples for FT-IR analyses

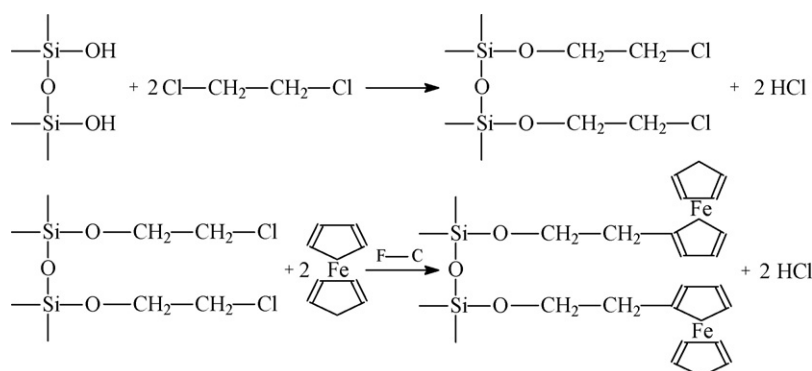


Fig. 2. Immobilization of ferrocene on silica gel.

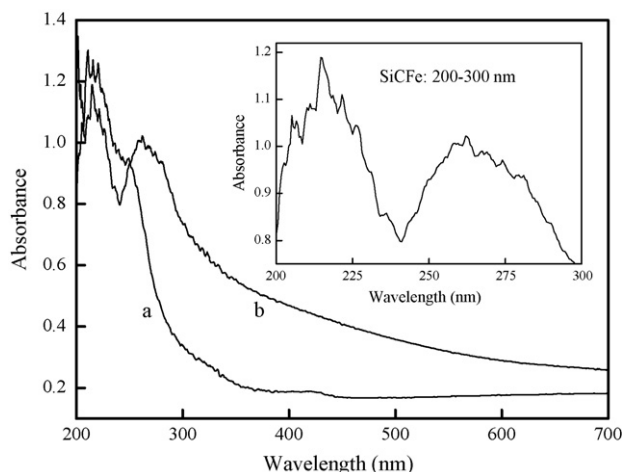


Fig. 3. Diffuse reflectance UV-vis spectra of the catalysts: (a) pure SiO_2 ; (b) SiCFe .

were prepared as follows: the suspensions at different irradiation time were filtered and the solution was evaporated below 50°C under reduced pressure. The residues together with KBr as a solid support were used for the IR measurements. Electron spin resonance (ESR) spectra were obtained using a Bruker model ESP 300E electron paramagnetic resonance spectrometer equipped with a quanta-Ray Nd:YAG laser system as the irradiation light source ($\lambda = 355\text{ nm}$). The settings were center field, 3480.00 G; microwave frequency, 9.79 GHz; power, 5.05 mW.

3. Results and discussion

3.1. Characterization of SiCFe catalyst

The diffuse reflectance UV-vis spectra (DRS) of different catalysts were recorded in Fig. 3 to investigate the nature of ferrocene supported on the silica. Comparing with pure SiO_2 (curve a), it can be found that the absorbance intensity of SiCFe in curve b was apparently enhanced from 700 to 300 nm. The main charge-transfer band at 215 nm was assigned to orbital located on the Cp ring [25], which appeared at the same positions as those reported for the ferrocene in solution. The bands at 240 nm [$(\text{Fe})e_{2g} \rightarrow (\text{Cp})e_{2u}$] and 265 nm [$(\text{Cp})e_{2u} \rightarrow (\text{Fe})e_{1g}$] corresponded to charge transfer between metal and Cp orbital, respectively [25], suggesting almost no change of the ferrocene metal-Cp distance. While the peaks at 194 and 197 nm were related to the unusually steric and electronic effects of the material [26].

As shown in Fig. 4, the infrared spectra of the catalyst also constituted an important source of information regarding of the character of the ferrocene immobilized on the functionalized silica gel. The peaks at 3440 and 970 cm^{-1} , assigned to O-H and Si-O stretching of the surface silanols of silica gel, respectively, almost disappeared after modification with dichloroethane [23]. In comparison with curve b (modification with dichloroethane), the characteristic peak at 1637 cm^{-1} related to the C=C vibration of Cp and another new strong peak at 1100 cm^{-1} of monosubstituted ferrocene [27] were displayed in curve c (SiCFe). All

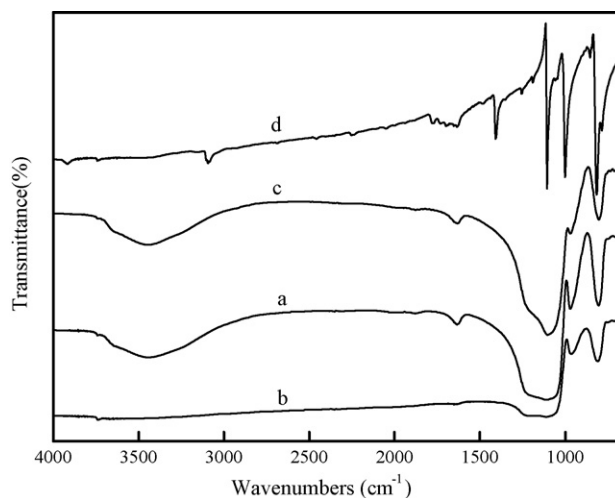


Fig. 4. FT-IR spectra of different samples: (a) pure SiO_2 ; (b) modified with dichloroethane; (c) SiCFe ; (d) ferrocene.

the results above indicated that ferrocene has been successfully anchored on the silica gel.

3.2. Photocatalytic degradation of ARB

3.2.1. Kinetic study of ARB photodegradation

ARB was used as a model pollutant to investigate the catalytic activity of SiCFe under different conditions when the initial solution pH was 3.0. As shown in Fig. 5, ARB was scarcely decolorized only in the presence of H_2O_2 (curve a), or UVA (curve b), as well as SiCFe and H_2O_2 in the dark (curve c); indicating that the degradation of ARB under these conditions was very limited. Although 54% of ARB was degraded because of the direct photolysis of hydrogen peroxide under UVA irradiation (curve d), it was interesting to found that 70% of ARB was decolorized after 120 min of reaction in the presence of SiCFe and UVA (curve e), indicating the catalyst could generate more reactive

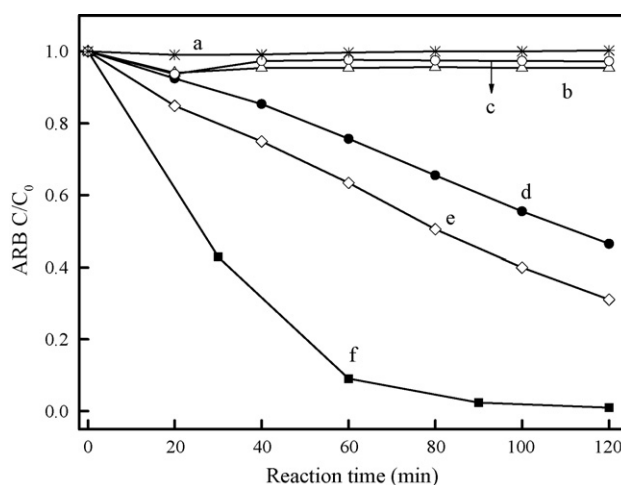


Fig. 5. Degradation of ARB under different conditions: (a) H_2O_2 ; (b) UVA; (c) $\text{SiCFe} + \text{H}_2\text{O}_2$; (d) $\text{H}_2\text{O}_2 + \text{UVA}$; (e) $\text{SiCFe} + \text{UVA}$; (f) $\text{SiCFe} + \text{UVA} + \text{H}_2\text{O}_2$. (Experimental conditions: pH=3.0, catalyst, 1 g l^{-1} ; ARB, 0.1 mM 50 ml; H_2O_2 , 13.8 mM .)

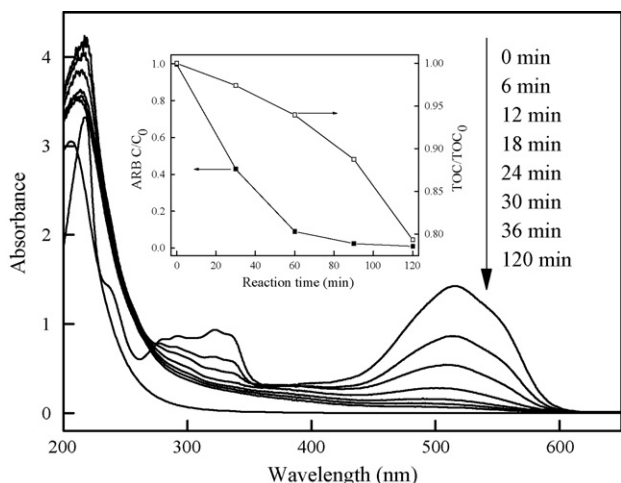


Fig. 6. UV-vis spectral changes of ARB as a function of irradiation time in the presence of SiCFe and H₂O₂ under UVA irradiation. The inset showed the TOC removal under the same conditions (experimental conditions: pH = 3.0, catalyst, 1 g l⁻¹; ARB, 0.1 mM 50 ml; H₂O₂, 13.8 mM).

oxygen species under UVA irradiation leading to the oxidative degradation of ARB. The concentration of ARB decreased much faster in the presence of SiCFe, UVA and H₂O₂ (curve f). It was because that in the later system the degradation of ARB came from the synergistic effect of the photocatalysis over SiCFe and the Fenton-like reaction in SiCFe/H₂O₂/UVA system.

The temporal absorption spectral changes of ARB under the optimum conditions at different irradiation times were displayed in Fig. 6. Azo structure of ARB at 514 nm (–N=N– group), as the most active site for oxidative attack [28], was destroyed rapidly and disappeared ultimately after 120 min reaction. Moreover, the characteristic peak at 320 nm in the UV region related to the naphthalene ring bonded to the –N=N– group in the dye molecule also decreased with the irradiation time, indicating that ARB was degraded into some aliphatic compounds, CO₂ and H₂O. This conjecture was further confirmed by the TOC removal during the photodegradation process. As shown in the inset of Fig. 6, TOC values dropped by about 21% after 120 min irradiation in the SiCFe/UVA/H₂O₂ system.

3.2.2. Stability of the catalyst

The durability of SiCFe was examined by recycling and then using the material under the same conditions above. SiCFe was recycled by a simple filtration and finally dried at 80 °C. The results were shown in Fig. 7. Clearly, no obvious deactivation of the catalyst in 4 successive cycles was observed when compared with the first cycle. The DRS spectrum of SiCFe after reaction was similar to that of the fresh catalyst (Fig. 8), indicating no obvious change in ferrocene of the catalyst. Besides that, the concentration of Fe leaching was 0.0357 mg l⁻¹ (AA-6300) and there was no free Fe²⁺ and Fe³⁺ existing in the solution based on the results of *O*-phenanthroline photometry [29] and Fe–ferron [30]. The results indicated that the covalent bond formed by Friedel–Crafts reaction between ferrocene and functionalized silica gel remarkably enhanced the chemical and physical stability of the catalyst.

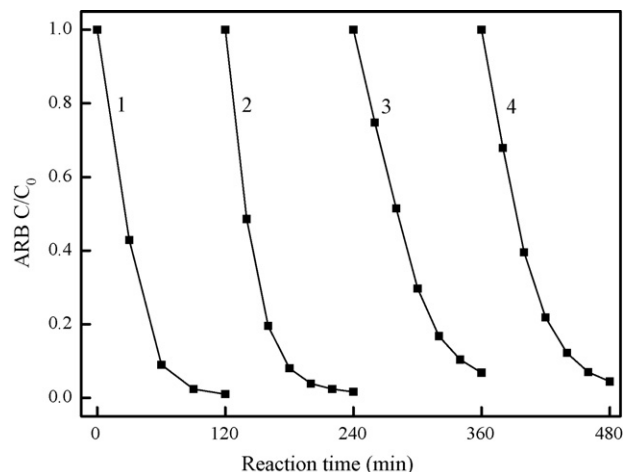


Fig. 7. Changes in the concentration of ARB during the multicycle photodegradation process in the presence of SiCFe and H₂O₂ under UVA irradiation (experimental conditions: pH = 3.0, catalyst, 1 g l⁻¹; ARB, 0.1 mM 50 ml; H₂O₂, 13.8 mM).

3.2.3. Effect of the initial solution pH

The solution pH could dramatically influence the degradation rate of organic compounds in the heterogeneous photocatalytic process. It was also an important operational parameter in actual wastewater treatment. Fig. 9 demonstrated the ARB concentration as a function of irradiation time when initial solution pH varied from 3 to 11. Obviously, the photodegradation of ARB in the SiCFe/H₂O₂/UVA system can operate efficiently in a wide range of pH. The catalyst exhibited better catalytic activity for the degradation of ARB at acidic pH than that at alkaline pH.

3.2.4. Effect of UV light wavelength

Fig. 10 depicted the effect of different UV light wavelength on the degradation rate of ARB. Obviously, ARB was scarcely decomposed in the dark (curve a), suggesting that the catalyst could not generate enough reactive oxygen species (ROS) without UV light irradiation. While in the presence of UV light, the

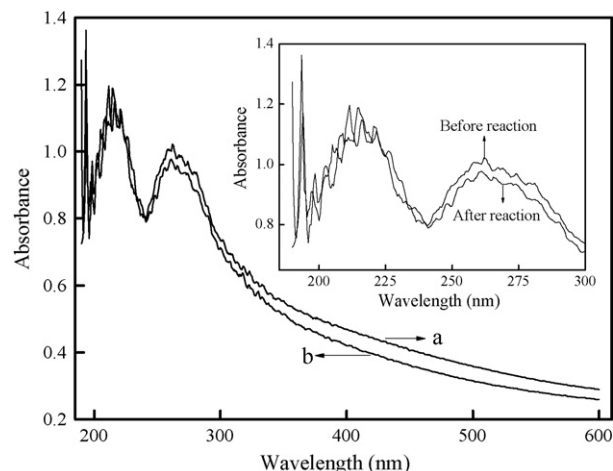


Fig. 8. Diffuse reflectance UV-vis spectra of the catalysts: (a) fresh catalyst; (b) after reused for 4 times.

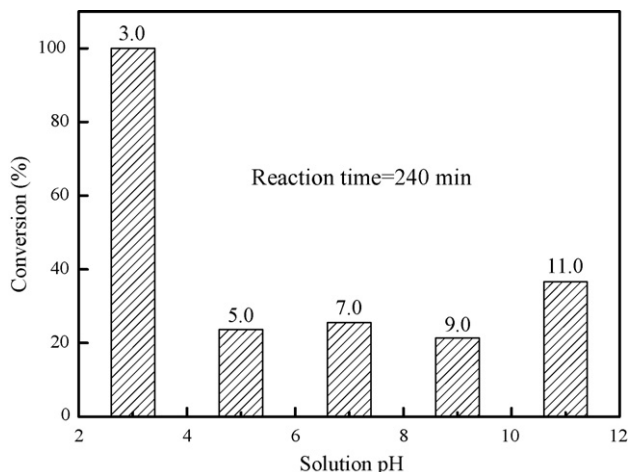


Fig. 9. Effect of solution pH on the degradation of ARB in the presence of SiCFe and H_2O_2 under UVA irradiation (experimental conditions: ARB, 0.1 mM 50 ml; catalyst, 1 g l⁻¹; 13.8 mM H_2O_2).

degradation of ARB was greatly accelerated (curves b and c), indicating that UV light had an important impact on the degradation of ARB. UV light in the SiCFe/ H_2O_2 /UV system played the roles of photoexcitation of ferrocene and photolysis of H_2O_2 , which led to the formation of ROS involved in the photodegradation process. In this experiment, UVC ($\lambda_{\text{max}} = 254$ nm) and UVA ($\lambda_{\text{max}} = 365$ nm) were used to investigate the effect of different UV light wavelength on the photodegradation of ARB. In comparison with curves b and c in Fig. 10, it was very clear that the degradation rate in the presence of UVC (30 min) was much faster than that irradiated by UVA (120 min), indicating that the UV light with a short wavelength was more effective in enhancing the degradation of ARB. According to the Refs. [31,32], the $\bullet\text{OH}$ quantum yield dramatically increased as the UV light wavelength decreased. The primary quantum yield of $\bullet\text{OH}$ radicals at 254 nm was reported to be 1.0, while the quantum yield at 360 nm was only 0.017. More $\bullet\text{OH}$ radicals increased sub-

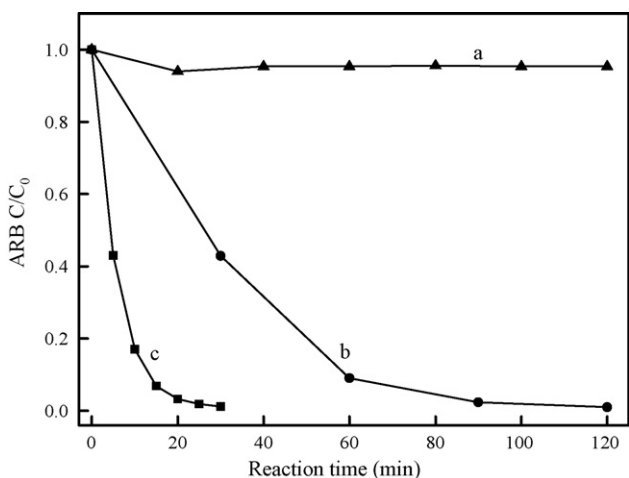


Fig. 10. Effect of UV light wavelength on the degradation of ARB: (a) in the dark; (b) under the irradiation of UVA ($\lambda_{\text{max}} = 365$ nm); (c) under the irradiation of UVC ($\lambda_{\text{max}} = 254$ nm). (Experimental conditions: pH = 3.0, catalyst, 1 g l⁻¹; ARB, 0.1 mM 50 ml; H_2O_2 , 13.8 mM.)

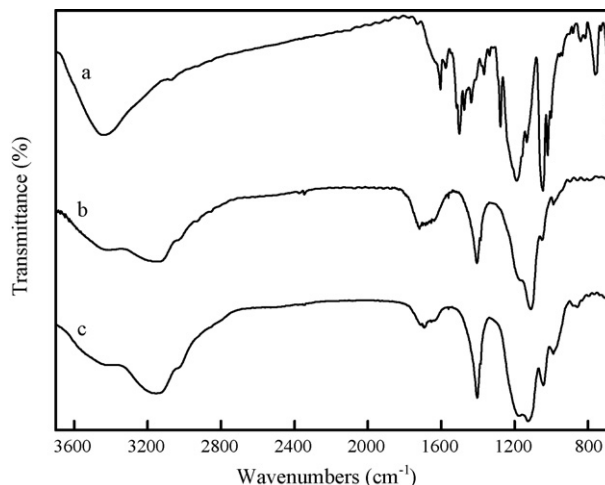


Fig. 11. Changes of FT-IR spectra during the photodegradation of ARB under UVA irradiation: (a) 0 min; (b) 80 min; (c) 120 min. (Experimental conditions: ARB, 0.1 mM 50 ml; catalyst, 1 g l⁻¹; 13.8 mM H_2O_2 .)

stantially with the decreasing UV light wavelength, then a much faster degradation of ARB was observed.

3.3. Mechanism of ARB photodegradation

3.3.1. FT-IR analysis of the intermediates in the degradation of ARB

The intermediates produced during the ARB degradation were examined with FT-IR and the infrared spectra were shown in Fig. 11. The peak intensities characteristic of the azo bond ($-\text{N}=\text{N}-$, at 1500 cm^{-1}) and the benzene ring ($1430\text{--}1600\text{ cm}^{-1}$) of ARB decreased with irradiation time [33]. The results indicated the disappearance of both the parental dye and its primary aromatic breakdown products. After irradiation for 120 min, the time required for complete decolorization of ARB, adsorption peak representing the $-\text{N}=\text{N}-$ bond disappeared. Meanwhile, the disappearance of peaks at 1190 and 1279 cm^{-1} of sulfonate and the increase of a new strong peak at 1127 cm^{-1} , characteristic absorption of SO_4^{2-} , with the irradiation time also proved the dye has been destroyed completely. At the same time, absorption peaks characteristic of the $\text{C}=\text{C}$ bond of alkenes at $1630\text{--}1692\text{ cm}^{-1}$ appeared, which were produced by the alkenes carboxylic acid. A new peak attributable to $\text{C}=\text{O}$ groups of carboxylic acids, aldehydes, and/or ketones, and a new wide peak for the $\text{O}-\text{H}$ of carboxylic acids appeared at 1720 and 3130 cm^{-1} , respectively. Associated with another new strong peak at 1405 cm^{-1} of carboxyl, it can be indicated that the benzene ring has been destroyed and some new carboxylic acids were formed during the photodegradation process of ARB.

3.3.2. Determination of radicals

The ESR technique was an effective method in identification of active radicals. For this study, all the ESR spectra were recorded in situ by laser irradiation ($\lambda = 355$ nm) using DMPO as the radical scavenger. In Fig. 12A, all the measured ESR spectra exhibited a 4-fold characteristic peak of $\text{DMPO}\cdot\text{OH}$ adducts with an intensity ratio of 1:2:2:1, indicating that $\bullet\text{OH}$ radicals

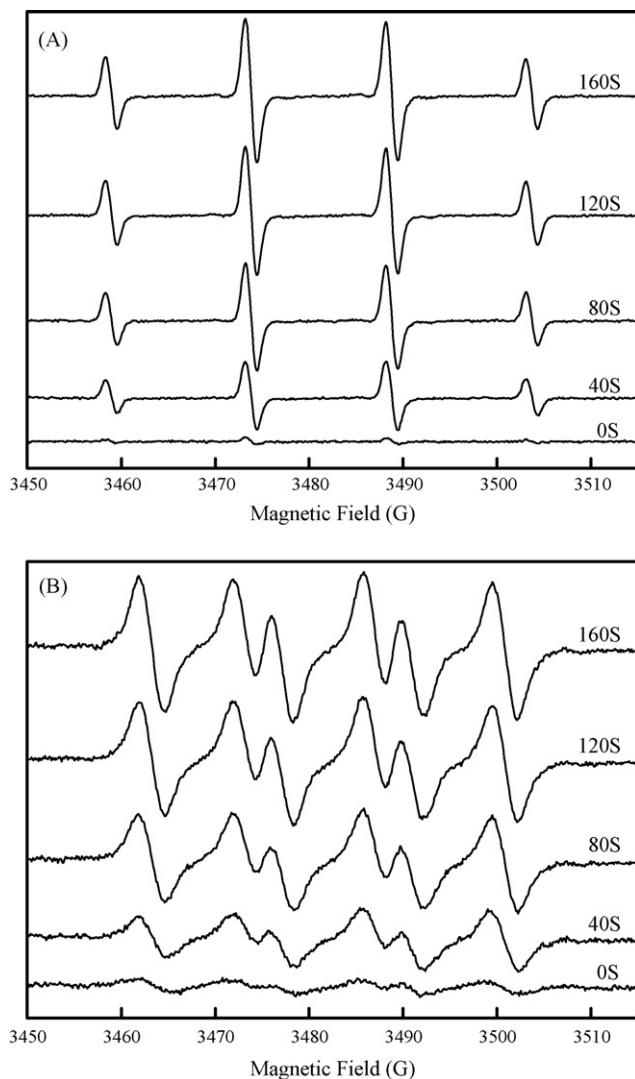


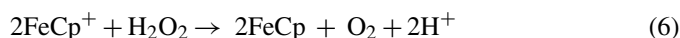
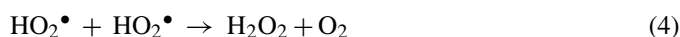
Fig. 12. DMPO spin-trapping ESR spectra recorded at ambient temperature in aqueous dispersion for DMPO-•OH (A) and in methanol dispersion for DMPO-HO₂•/O₂•⁻ (B) when SiCFe/H₂O₂ system was irradiated with UV ($\lambda = 355$ nm).

were generated and resulted in the photodegradation of ARB in SiCFe/H₂O₂/UVA system. The intensity of the four peaks of DMPO-•OH was significantly enhanced with increasing irradiation time. While the ESR signal of DMPO-•OH was not displayed in the dark, indicating that UV irradiation can effectively generate •OH radicals and accelerated significantly the degradation of ARB.

To verify whether •OH was the dominant ROS, the formation of HO₂•/O₂•⁻ radicals was also detected in methanol (Fig. 12B), since the HO₂•/O₂•⁻ radicals in water were very unstable and underwent facile disproportionation rather than slow reaction with DMPO [34]. Compared with the results conducted in the dark, the sextet peaks of DMPO-HO₂•/O₂•⁻ adducts were observed as expected, and the signal intensity increased apparently with irradiation time. Therefore, both •OH and HO₂•/O₂•⁻ radicals were the active species involved in the ARB photodegradation process.

3.3.3. Reaction mechanism discussion

A possible reaction mechanism was proposed based on the experimental results. It was reported that ferrocene could absorb UV light strongly [35,36]. So ferrocene immobilized on silica gel was first excited to generate electron-hole pairs under UVA irradiation and produced some radicals indirectly (Eqs. (1)–(5)).



While the formed FeCp⁺ was fairly stable in acid aqueous solution [37] and the recycling of FeCp⁺/FeCp (Eq. (5)) was then greatly inhibited. Therefore the degradation rate of ARB in SiCFe/UVA system was slower than that conducted in SiCFe/H₂O₂/UVA system. The addition of H₂O₂ may accelerate the conversion of FeCp⁺ to FeCp (Eq. (6)) and led to further generation of radicals according to Eqs. (5) and (7). Meanwhile, the enhanced recycling of FeCp⁺/FeCp greatly inhibited the leakage of Fe ion and prolonged the lifetime of SiCFe catalyst. The formation of •OH and HO₂•/O₂•⁻, as evidenced by ESR experiments, then react with the substrate adsorbed on the catalyst (Eq. (8)), leading to the decolorization and mineralization of ARB.

4. Conclusion

SiCFe was synthesized by covalent grafting of ferrocene on functionalized silica gel with a -C₂H₄- linkage. The catalyst exhibited a high catalytic activity and excellent long-term stability for the degradation of ARB in the presence of H₂O₂ and UVA. The good stability can be attributed to the covalent bond between ferrocene and silica gel, which can effectively decrease the Fe leaching from SiCFe to the solution. The initial solution pH and different UV light wavelength both have strong influences on the photocatalytic efficiency. The ESR technique has verified that both •OH and HO₂•/O₂•⁻ radicals were generated and participated in the ARB degradation process.

Acknowledgement

This work was supported by the National Natural Science Foundation of China (Nos. 50538090, 20377050, 20537020, 20577062).

References

- [1] J. Fernandez, P. Maruthamuthu, J. Kiwi, Photobleaching and mineralization of orange II by oxone and metal-ions involving Fenton-like chemistry under visible light, J. Photochem. Photobiol. A: Chem. 161 (2004) 185–192.

- [2] M.R. Hoffmann, S.T. Martin, W. Choi, D.W. Bahnemann, Environmental applications of semiconductor photocatalysis, *Chem. Rev.* 95 (1995) 69–96.
- [3] H. Fu, C. Pan, W. Yao, Y. Zhu, Visible-light-induced degradation of rhodamine B by nanosized Bi_2WO_6 , *J. Phys. Chem. B* 109 (2005) 22432–22439.
- [4] J. Li, W. Ma, Y. Huang, X. Tao, J. Zhao, Y. Xu, Oxidative degradation of organic pollutants utilizing molecular oxygen and visible light over a supported catalyst of $\text{Fe}(\text{bpy})_3^{2+}$ in water, *Appl. Catal. B: Environ.* 48 (2004) 17–24.
- [5] N. Quici, M.E. Morgada, G. Piperata, P. Babay, R.T. Gettar, M.I. Litter, Oxalic acid destruction at high concentrations by combined heterogeneous photocatalysis and photo-Fenton processes, *Catal. Today* 101 (2005) 253–260.
- [6] S. Campestrini, B. Meunier, Olefin epoxidation and alkane hydroxylation catalyzed by robust sulfonated manganese and iron porphyrins supported on cationic ion-exchange resins, *Inorg. Chem.* 31 (1992) 1999–2006.
- [7] S. Parra, V. Nadtochtenko, P. Albers, J. Kiwi, Discoloration of azo-dyes at biocompatible pH-values through an Fe-histidine complex immobilized on Nafion via Fenton-like processes, *J. Phys. Chem. B* 108 (14) (2004) 4439–4448.
- [8] A. Sorokin, J.L. Seris, B. Meunier, Efficient oxidative dechlorination and aromatic ring cleavage of chlorinated phenols catalyzed by iron sulfophthalocyanine, *Science* 28 (26) (1995) 1163–1166.
- [9] R.F. Parton, I.F.J. Vankelecom, M.J.A. Casselman, C.P. Bezoukhanova, J.B. Uytterhoeven, P.A. Jacobs, An efficient mimic of cytochrome P-450 from a zeolite-encaged iron complex in a polymer membrane, *Nature* 370 (18) (1994) 541–544.
- [10] L. Ji, X. Peng, J. Huang, Progress in study on metalloporphyrin mimicking metalloenzymes, *Prog. Natur. Sci.* 12 (5) (2002) 321–330.
- [11] W. Ma, J. Li, X. Tao, J. He, Y. Xu, J.C. Yu, J. Zhao, Efficient degradation of organic pollutants by using dioxygen activated by resin-exchanged iron (II) bipyridine under visible irradiation, *Angew. Chem. Int. Ed.* 42 (9) (2003) 1029–1032.
- [12] Y. Huang, W. Ma, J. Li, M. Cheng, J. Zhao, A novel β -CD-Hemin complex photocatalyst for efficient degradation of organic pollutants at neutral pHs under visible irradiation, *J. Phys. Chem. B* 107 (2003) 9409–9414.
- [13] M. Sanchez, N. Chap, J.B. Cazaux, B. Meunier, Metallophthalocyanines linked to organic copolymers as efficient oxidative supported catalysts, *Eur. J. Inorg. Chem.* 2001 (7) (2001) 1775–1783.
- [14] M. Alvaro, E. Carbonell, M. Espla, H. Garcia, Iron phthalocyanine supported on silica or encapsulated inside zeolite Y as solid photocatalysts for the degradation of phenols and sulfur heterocycles, *Appl. Catal. B: Environ.* 57 (2005) 37–42.
- [15] Y. Huang, J. Li, W. Ma, M. Cheng, J. Zhao, Efficient H_2O_2 oxidation of organic pollutants catalyzed by supported iron sulfophenylporphyrin under visible light irradiation, *J. Phys. Chem. B* 108 (2004) 7263–7270.
- [16] K. Deng, F. Huang, D. Wang, Z. Peng, Y. Zhou, A novel catalyst iron (II) tetra(1,4-dithin)porphyrine for oxygenating degradation of organic pollutants in aqueous solutions, *Chem. Lett.* 33 (2004) 34–35.
- [17] J. Li, W. Ma, Y. Huang, M. Cheng, J. Zhao, J.C. Yu, A highly selective photooxidation approach using O_2 in water catalyzed by iron(II) bipyridine complex supported on NaY zeolite, *Chem. Commun.* 17 (2003) 2214–2215.
- [18] K.J. Balkus Jr., A.K. Khanmamedova, K.M. Dixon, F. Bedioui, Oxidations catalyzed by zeolite ship-in-a-bottle complexes, *Appl. Catal. A: Gen.* 143 (1996) 159–173.
- [19] B. Shen, S. Ren, Q. Guo, Covalent grafting of zirconocene dichloride moiety on MCM-41, *Mol. Catal.* 18 (2004) 93–97.
- [20] M. Dabrowski, B. Misterkiewicz, A. Sporzynski, Solubilities of substituted ferrocenes in organic solvents, *J. Chem. Eng. Data* 46 (2001) 1627–1631.
- [21] H. Gulce, A. Gulce, M. Kavanoz, H. Coskun, A. Yildiz, A new amperometric enzyme electrode for alcohol determination, *Biosens. Bioelectron.* 17 (2002) 517–521.
- [22] Z. Yu, L. Qi, M. Qin, D. Guo, H. Wang, Decomposition mechanism of hydrogen peroxide catalyzed by ferrocene in toluene–ethanol mixed solution, *Appl. Chem.* 21 (2004) 41–44.
- [23] L. Li, J. Shi, J. Yan, X. Zhao, H. Chen, Mesoporous SBA-15 material functionalized with ferrocene group and its use as heterogeneous catalyst for benzene hydroxylation, *Appl. Catal. A: Gen.* 263 (2004) 213–217.
- [24] D.R. Burri, I.R. Shaikh, K.M. Choi, S.E. Park, Facile heterogenization of homogeneous ferrocene catalyst on SBA-15 and its hydroxylation activity, *Catal. Commun.* 8 (2007) 731–735.
- [25] L. Mohanambe, S. Vasudevan, Inclusion of ferrocene in a cyclodextrin-functionalized layered metal hydroxide: a new organometallic-organic-LDH nanohybrid, *Inorg. Chem.* 44 (7) (2005) 2128–2130.
- [26] W. Liu, The UV spectroscopy study on some ferrocenyl-formylferrocenylalkanes and derivatives, *J. Ningxia University (Natur. Sci. Ed.)* 17 (3) (1996) 70–73.
- [27] M. Osenbl, The structure and chemistry of ferrocene. IV. Intraannular resonance effects, *J. Am. Chem. Soc.* 81 (1959) 4530–4530.
- [28] N. Daneshvar, D. Salari, A.R. Khataee, Photocatalytic degradation of azo dye acid red 14 in water: investigation of the effect of operational parameters, *J. Photochem. Photobiol. A: Chem.* 157 (2003) 111–116.
- [29] State Environmental Protection Administration of China, Analytical Method of Water and Wastewater, fourth ed., Beijing, 2002, pp. 368–370.
- [30] D. Wang, Modified IPF-PFSi: Its Preparation, Characterization and Coagulation Behavior, Chinese Academy of Sciences, Beijing, 1997, p. 63.
- [31] S.F. Kang, C.H. Liao, H.P. Hung, Peroxidation treatment of dye manufacturing wastewater in the presence of ultraviolet light and ferrous ions, *J. Hazard. Mater. B* 65 (1999) 317–333.
- [32] B.C. Faust, J. Hoigne, Photolysis of Fe (III)-hydroxy complexes as sources of OH radicals in clouds, fog and rain, *Atmos. Environ. A* 24 (1990) 79–89.
- [33] C. Hu, J.C. Yu, Z. Hao, P.K. Wong, Photocatalytic degradation of triazine-containing azo dyes in aqueous TiO_2 suspensions, *Appl. Catal. B: Environ.* 42 (2003) 47–55.
- [34] W. Ma, Y. Huang, J. Li, M. Cheng, W. Song, J. Zhao, An efficient approach for the photodegradation of organic pollutants by immobilized iron ions at neutral pHs, *Chem. Commun.* 13 (2003) 1582–1583.
- [35] H. Yang, X. Chen, W. Jiang, Y. Lu, Convenient synthesis of new water-soluble monosubstituted functional ferrocene derivatives, *Inorg. Chem. Commun.* 8 (2005) 853–857.
- [36] T. Wang, J. Chen, Z. Li, P. Wan, Several ferrocenium salts as efficient photoinitiators and thermal initiators for cationic epoxy polymerization, *J. Photochem. Photobiol. A: Chem.* 187 (2007) 389–394.
- [37] Y.S. Sohn, D.N. Hendrickson, H.B. Gray, Electronic structure of metallocenes, *J. Am. Chem. Soc.* 93 (1971) 3603–3612.